

## Plasmons in a quasi-one-dimensional metal in the random-phase and screened-Hartree-Fock approximations

R. Liebmann,\* P. Lemke, and J. Appel

*I. Institut für Theoretische Physik, Universität Hamburg, Hamburg, Germany*

(Received 16 May 1977)

We consider plasmons in a lattice with chain structure. The electrons are treated in a one-band tight-binding model. From the corresponding longitudinal dielectric matrix  $\epsilon_{GG}(q, \omega)$  the plasmon dispersion is determined in the random-phase approximation and in the screened-Hartree-Fock approximation. In comparing these results we find a remarkable decrease of the short-wavelength part of the plasmon dispersion relative to the long-wavelength limit, caused by the exchange corrections. The inclusion of overlap matrix elements is important for bands which are not half-filled. Furthermore, this inclusion of overlap is a necessary but not sufficient precondition for the existence of a second "acoustical" plasmon branch in our model.

### I. INTRODUCTION

In recent years there has been great interest in quasi-one-dimensional metals, which in many respects behave quite different from usual metals. Two of the best known representatives of this class of substances are potassium cyano-platinate,  $K_2Pt(CN)_4Br_{0.3} \cdot 3H_2O$  (KCP), and tetrathiafulvalenium-tetracyanoquinodimethanide (TTF-TCNQ), both of which form crystals with chain structure. Unfortunately, the lattices of both of these compounds are very complex and, therefore, quantitative agreement between experiment and model calculation has not yet been achieved.

In general, the plasmon dispersion (apart from the polariton region  $\omega/|q| \geq c$  not treated here) is determined by the roots of the determinant of the frequency-dependent longitudinal dielectric function  $\epsilon_{GG}(q, \omega)$  which is a matrix in the reciprocal-lattice vectors. Williams and Bloch<sup>1,2</sup> (WB) and WB, Butler, and Rousseau<sup>3</sup> have investigated the plasmon dispersion of quasi-one-dimensional metals in several papers. They take full account of the local-field effects corresponding to the matrix character of  $\epsilon$ . They consider the electrons to be bound to the chains and to be localized or free along them. WB confine themselves to the time-dependent Hartree or random-phase approximation (RPA) for the dielectric matrix, neglecting the pertinent corrections due to exchange and correlation. Contrary to this assumption we calculate the dielectric function for tightly bound electrons in a simple form of the screened-Hartree-Fock (SHF) approximation which includes exchange effects and also to some extent correlation. In doing this we closely follow the formulation of Sham<sup>4</sup> and Hanke<sup>5</sup> in describing the contribution of exchange to the polarizability. The comparison of the resulting SHF plasmon dispersion with that of RPA shows that the main effect of exchange is to

decrease the short-wavelength part of the plasmon dispersion relative to the long-wavelength limit.

Inclusion of overlap matrix elements in the dielectric matrix, neglected by Williams and Bloch; may lead to a second root of the determinant of  $\epsilon_{GG}(q, \omega)$  for frequencies above the electron-hole continuum even in a one-band one-strand model. Yet the existence of this second root corresponding to an acoustical plasmon branch depends strongly on parameters such as the bandwidth, the radius of the atomic orbitals, and the Fermi wave vector.

### II. DIELECTRIC MATRIX AND PLASMON CONDITION

The model we use to determine the dielectric function is similar to the tight-binding model of Williams and Bloch. It is a special case of the general tight-binding formulation of the dielectric function.<sup>6</sup> We assume a simple tetragonal lattice with the lattice constant  $a_{\parallel}$  in chain direction considerably shorter than that in the two perpendicular directions  $a_{\perp}$ . The electrons are described in a one-band tight-binding model, the atomic orbitals are represented by isotropic Gaussian functions. The corresponding wave functions and energies in Hartree approximation are

$$\psi_{\mathbf{k}}(\mathbf{r}) = N^{-1/2} \sum_{\mathbf{l}} e^{i\mathbf{k}\cdot\mathbf{R}_{\mathbf{l}}} \phi(\mathbf{r} - \mathbf{R}_{\mathbf{l}}), \quad (2.1)$$

with

$$\phi(\mathbf{r}) = (2/\pi b^2)^{3/4} e^{-r^2/b^2}$$

and

$$E_{\mathbf{k}} = E_{\mathbf{k}_{\parallel}} = E_0 - E_1 \cos(k_{\parallel} a_{\parallel}). \quad (2.2)$$

$N$  is the number of atoms,  $\mathbf{R}_{\mathbf{l}}$  is a lattice vector,  $b$  is the radius of the Gaussian orbital. Since  $a_{\perp}$  is assumed to be large enough to make overlap between orbitals on different chains negligible,

the energy  $E_k$  depends only on the component of the wave vector parallel to the chains  $k_{\parallel}$ . It is just this negligible interchain overlap which renders the model quasi-one-dimensional. The corresponding RPA dielectric function is

$$\epsilon_{GG'}^{\text{RPA}}(q\omega) = \delta_{GG'} - v(q+G) \times \sum_{ss'} A^s(q+G) N^{ss'}(q\omega) A^{s'*}(q+G'), \quad (2.3)$$

with

$$v(q+G) = 4\pi e^2 / \Omega |q+G|^2, \quad (2.4)$$

$$A^s(q+G) = e^{iGR_s/2} \int dr^3 \phi\left(r - \frac{R_s}{2}\right) e^{-i(q+G)r} \times \phi\left(r + \frac{R_s}{2}\right), \quad (2.5)$$

and

$$N_{(q\omega)}^{ss'} = \frac{2}{N} \sum_k \frac{f_{k-q/2} - f_{k+q/2}}{E_{k-q/2} - E_{k+q/2} + \hbar\omega} e^{-ik(R_s - R_{s'})}. \quad (2.6)$$

$\Omega = a_{\parallel} a_{\perp}^2$  is the unit-cell volume,  $R_s$  is a lattice vector in chain direction. We took  $R_s = 0$ , we include nearest neighbors along the chains.  $f_k$  is the Fermi distribution function for the electron state with energy  $E_k$ .

In time-dependent Hartree-Fock (HF) approximation in principle three changes occur: (i) The exchange term of the self-energy  $\Sigma^x(k)$  must be added to the Hartree electron energy. (ii) In general the wave function will change, yet in our one-band tight-binding ansatz this change is ignored. We take the radius  $b$  of the atomic orbitals as an independent parameter. (iii) The polarizability  $N$  now contains a sum over internal Coulomb ladders.

The result for the exchange self-energy in our model is given by

$$\Sigma^x(k) = \Sigma^x(k_{\parallel}) = \sum_{s,s'} \cos(k_{\parallel} R_s) V_x^{ss'}(0) \times \frac{1}{N} \sum_{k'} f_{k'} \cos(k' R_{s'}), \quad (2.7)$$

where  $V_x^{ss'}(0)$  is the  $q=0$  value of the exchange Coulomb matrix

$$V_x^{ss'}(q) = \sum_m \exp[i(q/2)(2R_m + R_s - R_{s'})] \times \langle s+m, s' | 0, m \rangle; \quad (2.8)$$

$$\langle s+m, s' | 0, m \rangle = \int dr^3 dr^{3'} \phi^*(r+R_s+R_m) \times \phi(r+R_{s'}) v(r-r') \phi^*(r') \phi(r'+R_m).$$

The HF polarizability  $N_{\text{HF}}$  in matrix notation can

be expressed in terms of the same exchange Coulomb matrix,<sup>5</sup>

$$N_{\text{HF}}(q\omega) = N(q\omega) [1 + \frac{1}{2} V_x(q) N(q\omega)]^{-1}, \quad (2.9)$$

where  $N(q\omega)$  has the form of Eq. (2.6) with  $\Sigma^x$  added to the Hartree energies. We want to stress the importance on including both the exchange contribution to the self-energy and that corresponding to the ladder diagrams at the same time. If only one of these contributions is taken into account, the long-wavelength plasmon frequency, for instance, diverges.

We now proceed to the screened-Hartree-Fock approximation. In the SHF discussed by Baym and Kadanoff<sup>7</sup> the bare Coulomb interaction in  $\Sigma^x$  and in the internal Coulomb ladders of the polarizability has to be screened by a RPA dielectric function. In addition the polarizability contains more complicated diagrams. We confine ourselves to a simplified version of SHF, where these more complicated diagrams are neglected and where the internal RPA-screened interaction is replaced by a screened potential of Yukawa form

$$v^s(r-r') = v(r-r') e^{-\lambda|r-r'|}. \quad (2.10)$$

Therefore, in our model the only difference to the HF approximation consists in replacing  $v(r-r')$  in Eq. (2.8) by  $v^s(r-r')$  of Eq. (2.10). Equations (2.7) and (2.9) remain formally unchanged.

We now turn to the well-known equation defining the plasmon dispersion for  $|q| > \omega/c$  in a periodic lattice

$$\det[\epsilon_{GG'}(q\omega)] = 0. \quad (2.11)$$

Since the longitudinal dielectric function in the tight-binding approximation has a separable form, the determinant of the infinite matrix  $\epsilon_{GG'}$ , Eq. (2.3), can be transformed exactly<sup>8</sup>

$$\det[\epsilon_{GG'}(q\omega)] = \det\left(\delta_{ss'} - \sum_{s''} V_H^{ss''}(q) N^{s''s'}(q\omega)\right), \quad (2.12)$$

where  $V_H$  is the (Hartree) Coulomb matrix appearing also in the inversion procedure<sup>6</sup> for  $\epsilon_{GG'}$ ;  $V_H$  is given by

$$V_H^{ss'}(q) = \sum_G A^{s*}(q+G) v(q+G) A^{s'}(q+G). \quad (2.13)$$

We note, that  $V_H^{00}(q)$  is just the effective Coulomb interaction  $U(q)$  of WB.<sup>1</sup> The matrix on the right-hand side of Eq. (2.12) has the advantage of being finite. In our model, where  $R_s$  is restricted to nearest neighbors in chain direction,  $V_H$  and  $N$  are  $3 \times 3$  matrices, and the determinant (2.12) can be evaluated easily.

### III. PLASMON DISPERSION IN RPA

#### A. Normal branch

We first discuss the case most similar to WB,<sup>1</sup> namely, the RPA results without overlap ( $R_s = 0$ ). Then on the right-hand side of Eq. (2.12) the matrix reduces to a scalar function. For simplicity we choose  $q$  always parallel to the chains. Then expansion for small  $q_{\parallel}$  yields

$$\omega_p^2(q_{\parallel}) = \omega_p^2(0) + \left[ \left( \frac{v_F}{a_{\parallel}} \right)^2 + \left( f - \frac{1}{12} \right) \omega_p^2(0) \right] (q_{\parallel} a_{\parallel})^2, \quad (3.1)$$

where

$$f = \lim_{q_{\parallel} \rightarrow 0} \left[ \left( [A^0(q_{\parallel})]^2 - 1 + \sum_{G \neq 0} \frac{|q_{\parallel}|^2}{|q_{\parallel} + G|^2} [A^0(q_{\parallel} + G)]^2 \right) / (q_{\parallel} a_{\parallel})^2 \right]. \quad (3.2)$$

Equation (3.1) differs from the result of WB by the constant  $f$ , proportional to the second derivative of  $V_H^{00}(q)$ . This constant  $f$  makes the quadratic term in (3.1) dependent on the radius of the localized electron orbitals. Inserting the Gaussian function, Eq. (2.1),  $f$  becomes a monotonous function of  $b$  which decreases with increasing orbital radius  $b$ . This lowering of the plasmon dispersion with increasing value of  $b$  is not restricted to small wave vectors where the expansion (3.1) is valid. For all  $q \neq 0$ ,  $V_H^{00}(q)$  decreases with increasing  $b$ , thus  $N^{00}(q\omega)$  must increase to satisfy Eq. (2.11) and, therefore, the plasmon dispersion is lowered. In Fig. 1 the dependence of the plasmon dispersion on  $b$  is shown for a half-filled band with bandwidth  $E_1 = 0.018$  Ry. The orbital radius  $b$  is  $2.7a_B$ ,  $3.0a_B$ , and  $3.5a_B$  (Bohr units), respectively. The lattice constants are  $a_{\parallel} = 6a_B$  and  $a_{\perp} = 16a_B$ , similar to the Pt sublattice in KCP. The comparison of the  $\theta = 0^\circ$  dispersion curves of Figs. 5 and 6 of WB<sup>1</sup> shows the same lowering for other model parameters.

We now include overlap matrix elements  $A^{\pm 1}(q + G)$ . The resulting plasmon dispersions for  $k_F = \frac{1}{6}\pi/a_{\parallel}$ ,  $\frac{1}{2}\pi/a_{\parallel}$ , and  $\frac{5}{6}\pi/a_{\parallel}$  are shown in Fig. 2, where all curves are normalized to unity for  $q = 0$  to eliminate the  $k_F$  dependence of the long-wavelength plasmon frequency. For the half-filled band the dispersion remains almost unchanged as compared to Fig. 1. But the difference between the two other curves corresponding to  $k_F = (\frac{1}{2} \pm \frac{1}{3})\pi/a_{\parallel}$  is entirely due to the overlap matrix elements. We note the fact that the Gaussian orbitals centered at nearest-neighbor sites are not orthogonal to one another. This nonorthogonality would lead to spur-

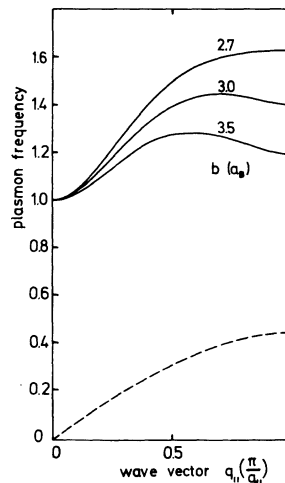


FIG. 1. Lowering of the RPA plasmon dispersion for increased values of the orbital radius:  $b = 2.7a_B$ ,  $b = 3.0a_B$ ,  $b = 3.5a_B$ .  $k_F = \frac{1}{2}\pi/a_{\parallel}$ ,  $E_1 = 0.018$  Ry. The dashed curve is the upper bound of the electron-hole region.

ious changes in the RPA long-wavelength plasmon frequency particularly for  $k_F \neq \frac{1}{2}\pi/a_{\parallel}$ , since then  $N^{01}(q\omega)$  does not vanish. Orthogonality requires that

$$\int dr^3 \phi^*(r) \phi(r + R_{\pm 1}) \equiv A^{\pm 1}(0) = 0. \quad (3.3)$$

We take account of this condition in an approximate manner by multiplying  $A^{\pm 1}(q + G)$  with the factor  $|q + G|^2 / (|q + G|^2 + p^2)$ . In Fig. 2 we take  $p = 2a_B^{-1}$ . Increasing  $p$  decreases the influence of the overlap elements and, therefore, reduces the difference between the dispersion curves for  $k_F = \frac{1}{2}\pi/a_{\parallel} \pm x$ . Due to the approximate orthogonalization the dispersion curves for  $k_F \neq \frac{1}{2}\pi/a_{\parallel}$  have a tentative character. They demonstrate, however, the importance of overlap matrix elements for bands not half-filled.

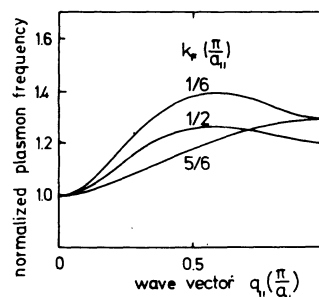


FIG. 2. Normalized plasmon dispersion with overlap matrix elements for three values of the Fermi wave vector:  $k_F = \frac{1}{6}\pi/a_{\parallel}$ ,  $k_F = \frac{1}{2}\pi/a_{\parallel}$ , and  $k_F = \frac{5}{6}\pi/a_{\parallel}$ .  $b = 3.5a_B$ ,  $p = 2a_B^{-1}$ ,  $E_1 = 0.018$  Ry.

### B. Acoustical plasmon branch in RPA

The inclusion of overlap matrix elements has another interesting consequence. In our nearest-neighbor model Eq. (2.11) can be written in a particularly simple form for the value  $q_1 = (\pi/a_n, 0, 0)$ . Then  $V^{01}$  and  $N^{01}$  are zero and we get

$$(1 - V_H^{00}(q_1)\bar{N}^{00}(q_1\omega))(1 - V_H^{11}(q_1)\bar{N}^{11}(q_1\omega)) = 0, \quad (3.4)$$

where

$$\bar{N}^{00}(q_1\omega) = N_{\text{RPA}}^{00}(q_1\omega),$$

and

$$\bar{N}^{11}(q_1\omega) = 2 \text{Re}[N_{\text{RPA}}^{11}(q_1\omega) + N_{\text{RPA}}^{*11}(q_1\omega)].$$

Obviously Eq. (3.4) can have two solutions. The frequency  $\omega_1$  for which the first factor on the left-hand side is zero leads to the plasmon already discussed. This solution exists for all values of the model parameters. In the second factor the term  $V_H^{11}$  is positive, but considerably smaller than  $V_H^{00}$ .  $\bar{N}^{11}$  is positive, but it remains finite for  $\hbar\omega \rightarrow 2E_1$  unlike  $\bar{N}^{00}$  which diverges in this limit. Therefore, the product  $V_H^{11}\bar{N}^{11}$  is limited for  $\hbar\omega \rightarrow 2E_1$ . A second solution  $\omega_2$  exists only for parameters such that the product  $V_H^{11}\bar{N}^{11}$  is greater 1 for  $\hbar\omega = 2E_1$  and then  $\omega_2$  will be much smaller than  $\omega_1$ . The determinant (2.12) cannot be factorized for general values of  $q$  and has to be calculated numerically. Figure 3 shows an example for this second plasmon branch for a half-filled band with parameters favorable for the existence of the second solution:  $E_1 = 0.004$  Ry,  $b = 4.1a_B$ ,  $p = 0.5a_B^{-1}$ . With decreasing wave vector the dispersion approaches asymptotically the electron-hole excitation region delimited by the dashed curve. For less favorable parameters, e.g., for greater bandwidth  $E_1$ , the acoustical branch does no longer exist above the electron-hole excitation region for all values of  $q_n$  or even may be absent completely.

The physics of the two dispersion branches is

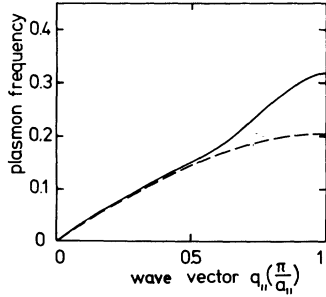


FIG. 3. Acoustical branch of the RPA plasmon dispersion.  $k_F = \frac{1}{2} \pi/a_n$ ,  $b = 4.1a_B$ ,  $p = 0.5a_B^{-1}$ ,  $E_1 = 0.004$  Ry. The dashed curve is the upper bound of the electron-hole region.

quite simple. In the tight-binding approximation density waves

$$\delta\rho_q(r) \propto \sum_k \psi_k(r) \psi_{k+q}^*(r)$$

can be split into contributions  $|\varphi(r - R_i)|^2$  and  $\varphi(r - R_i)\varphi^*(r - R_{i\pm 1})$ , the Fourier transforms of which are  $A^0(q+G)$  and  $A^{\pm 1}(q+G)$ , respectively. They correspond to the parts of the electron density localized around the atoms and around the middle between nearest neighbors. For  $q$  at the Brillouin-zone boundary there are two possible collective density modes. In the first mode the density at nearest-neighbor atoms oscillates with opposite phase and does not change between them. In the second mode the density oscillates between the atoms and is constant at the atom sites. These two modes, which do not couple, are the optical and the acoustical plasmon for  $q = q_1$ . Yet we note that we can make no general statement on the existence of the acoustical plasmon branch, since this would require a really consistent calculation of the band structure and the wave functions.

### IV. PLASMONS IN SHF APPROXIMATION

We now discuss the effect of screened exchange contributions on the plasmon dispersion. Since a calculation of  $V_x^{ss'}$ , Eq. (2.6), is difficult even with a screened potential of Yukawa form and since we are interested only in qualitative changes, we calculate the matrix elements  $V_x^{ss'}$  with a bare Coulomb potential and multiply them by factors  $e^{-\lambda\bar{r}_{ss'}}$ . The parameters  $\bar{r}_{ss'}$  are the estimated mean distances between local densities  $\rho(r)$  and  $p(r')$ , and  $\lambda$  is the screening parameter. Again we take account of the nonorthogonality of the Gaussian functions approximately by reducing the matrix elements  $\langle 10|00 \rangle$  and  $\langle 10|10 \rangle$  by factors  $\frac{1}{3}$  and  $\frac{1}{5}$ , respectively. The elements  $\langle 00|00 \rangle$  and  $\langle 11|00 \rangle$  de-

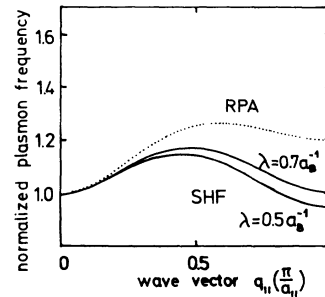


FIG. 4. Full curves: Normalized SHF plasmon dispersion for two values of the screening parameter:  $\lambda = 0.7a_B^{-1}$  and  $\lambda = 0.5a_B^{-1}$ .  $k_F = \frac{1}{2} \pi/a_n$ . The other parameters are as in Fig. 2. The dotted curve is the corresponding RPA dispersion.

pend only slightly on incomplete orthogonalization and are not reduced. In Fig. 4 the full curves show the resulting plasmon dispersions in SHF for the two values of the screening parameter,  $\lambda = 0.7\alpha_B^{-1}$  and  $\lambda = 0.5\alpha_B^{-1}$ . All of the other parameters are the same as in Fig. 2; therefore, overlap elements are included. The dotted curve is the corresponding RPA dispersion. For better comparison we have normalized all three dispersions to unity for  $q=0$ . We note that in our SHF model  $\omega_p(0)$  is up to 40% larger than in RPA. As Fig. 4 shows, the main effect of including screened exchange is to lower the short-wavelength part of the dispersion relative to the long-wavelength limit. This result is remarkably independent of the model parameters. The lowering can be understood in terms of a simplified model, where the overlap is neglected and only the largest matrix elements  $V_H^{00}$  and  $V_x^{00}$  are taken into account. Then proceeding from RPA to SHF the only change is the reduction of  $V_H^{00}$  to  $V_H^{00} - V_x^{00}$ ; and the resulting shift of the plasmon dispersion to lower frequencies is similar to the effect of an increased orbital radius  $b$  in RPA (cf. Fig. 1). The other matrix elements, particularly those of  $V_x^{ss'}$ , cause considerable changes

of the dispersion. Figure 4 demonstrates, however, that the inclusion of the overlap matrix elements does not change this simple consideration of the effect of exchange too much, after the resulting general shift of the dispersion is eliminated by normalizing with the corresponding long-wavelength limit.

## V. CONCLUSION

We have investigated the effect of the overlap matrix elements and of screened exchange on the plasmon dispersion of a one-band tight-binding model of a quasi-one-dimensional conductor. This model is certainly too simple to allow for a quantitative comparison with experiments, because the two main representatives of one-dimensional metals both have rather complicated lattices. Therefore, wave functions and band structure will be much more complicated than in our model. Nevertheless we think, the importance of overlap matrix elements for bands not half-filled (as in KCP) and particularly of screened exchange corrections to the plasmon dispersion, cf. Figs. 1, 2, and 4, is not restricted to our special model, but will be a rather general feature.

---

\*Present address: Cornell University, Laboratory of Atomic and Solid State Physics, Ithaca, N.Y. 14853.

<sup>1</sup>P. F. Williams, and A. N. Bloch, Phys. Rev. B 10, 1097 (1974).

<sup>2</sup>P. F. Williams and A. N. Bloch, Phys. Rev. Lett. 36, 64 (1976).

<sup>3</sup>P. F. Williams, M. A. Butler, D. L. Rousseau, and A. N. Bloch, Phys. Rev. B 10, 1109 (1974).

<sup>4</sup>L. J. Sham, Phys. Rev. B 6, 3584 (1972).

<sup>5</sup>W. R. Hanke, Phys. Rev. B 8, 4591 (1973); in more detail, W. Hanke and L. J. Sham, *ibid.* 12, 4501 (1975).

<sup>6</sup>W. R. Hanke, Phys. Rev. B 8, 4585 (1973).

<sup>7</sup>G. Baym and L. P. Kadanoff, Phys. Rev. 124, 287 (1961).

<sup>8</sup>G. Zielke, *Numerische Berechnung von benachbarten inversen Matrizen* (Vieweg, Braunschweig, 1970).